

## Highlights

### **Reducing RES Droughts through the integration of wind and Solar PV**

Boris Morin, Aina Maimó Far, Damian Flynn, Conor Sweeney

- RES droughts are analysed using 45 years of hourly wind and solar PV generation data
- RES droughts from C3S-Energy and ERA5-Atlite datasets are compared
- Adding solar PV to a wind-dominated system reduces RES drought frequency and duration
- Validated RES datasets are crucial to accurately identify RES drought extremes

# Reducing RES Droughts through the integration of wind and Solar PV

Boris Morin<sup>a,\*</sup>, Aina Maimó Far<sup>a</sup>, Damian Flynn<sup>b</sup>, Conor Sweeney<sup>a</sup>

*<sup>a</sup>School of Mathematics and Statistics, University College Dublin, Belfield, Dublin  
4, Dublin, D04 V1W8, Ireland*

*<sup>b</sup>School of Electrical and Electronic Engineering, University College Dublin, Belfield,  
Dublin 4, Dublin, D04 V1W8, Ireland*

---

\*Corresponding author

*Email addresses:* `boris.morin@ucdconnect.ie` (Boris Morin ),  
`aina.maimofar@ucd.ie` (Aina Maimó Far), `damian.flynn@ucd.ie` (Damian Flynn),  
`conor.sweeney@ucd.ie` (Conor Sweeney)

---

## Abstract

Increasing the share of electricity produced from renewable energy sources (RES), combined with RES dependence on weather, poses a critical challenge for energy systems. This study investigates the importance of the balance between wind and solar photovoltaic (PV) capacity on periods of low renewable generation, known as RES droughts. Three different RES models are used to estimate the capacity factors for different scenarios of installed capacities for wind and solar PV power. The skill of the RES models is quantified by comparing capacity factor time series to observed hourly data and by assessing their representation of observed RES droughts. The RES models are used to generate a 45-year hourly time series of RES capacity factor, enabling analysis of the frequency, duration and return periods of RES droughts at a climatological scale. Results show the importance of using an accurate, validated RES model for RES drought risk assessment. The addition of solar PV capacity to a wind-dominated system results in a significant reduction in the frequency and duration of RES droughts, while also reducing extremes and seasonal drought patterns. These findings underscore the importance of diversification in RES capacity to enhance energy security and resilience.

*Keywords:* RES Drought, Wind Power, Solar PV Power, Renewable Energy Sources, Return Periods

---

## 1. Introduction

The EU aims to generate at least 69% of its electricity from renewable energy sources (RES) by 2030, up from 41% in 2022 [1]. While this transition is essential for reducing greenhouse gas emissions, it also highlights the challenge of managing the variability of weather-dependent energy sources such as wind and solar photovoltaic (PV) power. This challenge is amplified by the increasing electrification of energy sectors, which places greater demand on the power system and makes it more sensitive to meteorological conditions, both in historical [2] and future climates [3]. Periods of low renewable generation, known as *Dunkelflaute* or RES droughts, pose significant risks to system adequacy and energy security, emphasising the need for a resilient energy system to meet both growing electricity demand and decarbonisation targets.

14 This study focuses on Ireland, a region with a strong reliance on wind  
15 power, which has ambitious targets for solar PV power expansion. This case  
16 study provides valuable insights into the potential benefits of diversifying  
17 the renewable energy mix on RES droughts. The performance of different  
18 RES datasets are compared, and a 45-year time series of RES generation is  
19 produced. The results highlight the role of increased solar PV capacity in  
20 reducing RES drought risks, offering insights for policymakers and energy  
21 planners.

22 Various approaches have been proposed in the literature to define and  
23 quantify RES drought events. One common method defines a RES drought  
24 as a period during which the average capacity factor (CF) remains below  
25 a fixed threshold for a specified duration. For example, Kaspar et al. [4]  
26 investigated the shortfall risks of low wind and solar PV generation in Europe,  
27 focusing on Germany, while Mockert et al. [5] extended this work to examine  
28 the link between weather regimes and RES droughts. Similar fixed-threshold  
29 approaches have also been applied using machine learning in regions such as  
30 Japan [6] and Hungary [7].

31 Alternative methods adjust the CF threshold dynamically over the year  
32 to account for seasonal variations in renewable production. Raynaud et al. [8]  
33 defined droughts as sequences of days with energy production below a thresh-  
34 old that varies seasonally, a methodology later adapted for India [9]. Build-  
35 ing on this, Kapica et al. [10] compared the likelihood of increased RES  
36 droughts in Europe under different climate models. Other studies have de-  
37 fined droughts based on deviations from daily mean production, as done  
38 by Rinaldi et al. [11] in the U.S. Western Interconnection, while Brown et  
39 al. [12] examined weekly timescales to explore meteorological influences. An-  
40 other method defines energy drought indices based on metrics commonly  
41 used in hydro-meteorology to characterise RES droughts [13]. This approach  
42 identifies periods of unusually low generation relative to historical production  
43 levels, using the lowest production percentiles. It has been applied in other  
44 studies, including analyses of RES droughts in the U.S. [14] and China [15].

45 In addition to examining periods of low renewable electricity generation,  
46 Raynaud et al. [8] analysed the imbalance between electricity demand and  
47 renewable generation, known as residual load. These events were studied  
48 alongside low-generation periods to assess their correlation. Similar analyses  
49 have been conducted in Europe [13] and the U.S. [14], revealing differing  
50 results across regions.

51 In this paper, the focus is exclusively on renewable electricity generation,

and a fixed threshold approach to define RES droughts is used, which facilitates consistent inter-comparison between scenarios with different installed wind and solar PV capacities.

RES droughts are identified using onshore wind and solar PV CF time series. In this study, three different datasets are used, all of which are driven by ERA5 data [16]. Two of the datasets are part of C3S Energy (C3S-E), an energy-based operational dataset produced by the EU Copernicus Climate Change Service [17]. One of the C3S-E datasets provides CF time series aggregated at the national scale, while the other provides the CF time series at each grid point, at the ERA5 resolution of  $0.25^\circ$ . The third dataset was generated using the Atlite model [18], which converts the ERA5 atmospheric data to a generation time series using specified wind turbine and PV panel models. Atlite is an open-source tool developed by PyPSA [18] and has been used for estimating wind and solar PV generation in order to study RES droughts [5].

The aim of this study is to answer two questions which could help on the decision making for the planning of reserve capacity in real case wind-dominated renewable energy system:

- What is the impact of selecting different modelling assumptions on the analysis of RES droughts?
- How does the integration of solar PV into a predominantly wind-based system alter the characteristics of RES droughts in a real-case setting?

The datasets used in this study are detailed in section 2, which describes their characteristics and relevance for evaluating RES droughts. Section 3 outlines the RES datasets used to simulate wind and solar PV generation and provides the methodology for defining and identifying RES drought events, including the thresholds and metrics applied. In section 4, the datasets are first verified against observed energy data to assess their accuracy, followed by an analysis of RES drought occurrences for two scenarios with different ratios of installed wind to solar PV capacities. Finally, section 5 offers a discussion of the results in the context of energy reliability and future planning, followed by the main conclusions and recommendations for further research.

## 2. Data

This study uses publicly available datasets to construct and validate the datasets for estimating the CF of wind and solar PV power. The primary

87 data sources include: EirGrid and SONI, the transmission system operators  
88 (TSO) for the Republic of Ireland and Northern Ireland, respectively; the  
89 ERA5 reanalysis dataset; and the C3S-E datasets.

### 90 *2.1. Wind and solar PV Capacity and Availability*

91 EirGrid, the TSO for the Republic of Ireland, and SONI, the Northern  
92 Ireland TSO, provide detailed datasets on all wind and solar PV farms across  
93 the island of Ireland (Republic of Ireland and Northern Ireland) from 1990  
94 to the present [19]. These datasets include information such as each farm’s  
95 installed capacity, name, and connection date. To enhance the accuracy of  
96 this data, the longitude and latitude for each farm were manually determined  
97 through online searches. For simplicity, this data will be referred to as orig-  
98 inating from EirGrid, as all-island data was directly obtained from EirGrid,  
99 and the combined regions of the Republic of Ireland and Northern Ireland  
100 will be referred to as Ireland throughout the remainder of this document.

101 The spreadsheet available from the EirGrid website contains two key vari-  
102 ables: generation and availability. Generation is the energy that a RES farm  
103 actually contributed to the grid, which may include limitations introduced  
104 by the TSO to maintain grid stability, such as constraints and curtailment.  
105 Availability represents the energy that would have been generated from a RES  
106 farm if no grid constraints had been applied, making it representative of the  
107 weather-related response. Generation and availability values are available  
108 from 2014 onward for wind power and from 2018 onward for solar PV power,  
109 although solar PV availability data only became present in the Republic of  
110 Ireland in 2023. This study focuses on availability for all analyses.

### 111 *2.2. Atmospheric Variables*

112 Atlite and C3S-E datasets are driven by the ERA5 reanalysis [16], pro-  
113 duced by the European Centre for Medium-Range Weather Forecasts (ECMWF).  
114 This global gridded dataset provides hourly atmospheric variables from 1940  
115 to the present at a horizontal resolution of  $0.25^\circ$ . It has proven to be the best  
116 choice for studying renewable energy in Ireland [20]. Table 1 lists the ERA5  
117 variables used by Atlite and C3S-Energy.

### 118 *2.3. C3S Energy*

119 The EU Copernicus Climate Change Service developed the C3S-E renew-  
120 able energy dataset for Europe [17], using ERA5 atmospheric variables and  
121 weather-to-energy models. This dataset provides hourly CF for wind and

Table 1: ERA5 variables used to calculate wind and solar PV generation

ERA5 name	variable
100 metre zonal and meridional wind speed	$u_{100}, v_{100}$
2 metre temperature	$t2m$
Surface net solar radiation	$ssr$
Surface solar radiation downwards	$ssrd$
Top of atmosphere incident radiation	$tisr$
Total sky direct solar radiation at surface	$fdir$

122 solar PV energy from 1979 to the present. The data are available on the  
 123 same grid as the ERA5 data, which has a horizontal resolution of  $0.25^\circ$ . The  
 124 time series are also available for download at two aggregated scales: regional  
 125 (NUTS 2) and national.

126 The wind CF in the C3S-E model is calculated using wind speeds at 100  
 127 metres ( $u_{100}, v_{100}$ ) and a standard turbine model, the Vestas V136/3450,  
 128 with a fixed hub height of 100 meters. This choice reflects trends in wind  
 129 turbine installations and was guided by expert recommendations. Since real-  
 130 time data on the exact wind turbine fleet across Europe is difficult to obtain,  
 131 C3S-E assumes a homogeneous distribution of turbines across the ERA5 grid.  
 132 While this approach does not capture the precise capacity factors reported  
 133 by grid operators, it provides a well-correlated time series that effectively  
 134 represents the impact of climate variability on wind power generation. The  
 135 turbine power curves used in the model are sourced from publicly available  
 136 databases, ensuring consistency with industry standards. The solar PV CF  
 137 in the C3S-E model is calculated at the grid level and represents the aggre-  
 138 gated output of all solar PV systems within each pixel, rather than a single  
 139 installation. It is derived from meteorological data, including surface solar  
 140 radiation downwards ( $ssrd$ ) and air temperature ( $t2m$ ), using a reference  
 141 solar PV plant model. This model incorporates empirical calculations for  
 142 key system components such as optical losses, module efficiency, and invert-  
 143 ers. The final CF accounts for a mix of module orientations typical for each  
 144 location [21].

### 145 3. Methods

146 This study uses three datasets to analyse RES droughts across the island  
 147 of Ireland. Data downloaded from C3S-E were used to obtain two datasets:

one based on national-level data (C3S-E N), and another on grid-level data (C3S-E G). The third dataset was computed using the Atlite model (Atlite).

### 3.1. C3S-Energy National

For national-level analyses, the inputs for this dataset are the aggregated CF time series provided by C3S-E at two levels: Republic of Ireland (NUTS0: IE) and Northern Ireland (NUTS2: UKN0). These values are based on the assumption that RES generation occurs at every ERA5 grid point in Ireland. A weighted average is computed to represent the total CF for the country.

### 3.2. C3S-E Gridded

For the gridded dataset, the inputs consist of the CF time series from C3S-E, along with the location of individual RES farms across Ireland. Using these inputs, the nearest grid point on the C3S-E dataset was identified for each farm, and the corresponding CF values were retrieved. A weighted average, based on installed capacity, was then computed to construct a CF time series that accounts for the actual spatial distribution of wind and solar PV farms in Ireland.

### 3.3. Atlite

For the Atlite dataset, the inputs include the locations of RES farms and ERA5 weather variables, such as wind speed at 100 metres ( $u_{100}$ ,  $v_{100}$ ) for wind generation, and radiation variables ( $ssr$ ,  $ssrd$ ,  $tisr$ , and  $fdir$ ) along with air temperature ( $t2m$ ) for solar PV generation. The meteorological inputs are processed using the Atlite model to estimate CF time series for wind and solar PV, incorporating specific characteristics such as wind turbines power curve and PV panel model. A key distinction between C3S-E and Atlite lies in their representation of wind turbines and PV panels. This study identifies the most appropriate wind turbine power curve to use from the 121 power curves made available by Renewables.ninja [22]. The selection of a specific wind turbine and PV panel characteristics is further discussed and explained in section 4.1.

### 3.4. Energy Scenarios

The output of those three datasets are one CF time series for both wind and Solar PV. In addition to analysing wind and solar PV generation separately, a combined CF was computed for each dataset by averaging wind and solar PV generation, weighted by their installed capacities at the end of



2023 (5.9 GW for wind power and 0.6 GW for solar PV power). This configuration is referred to as the 91W-9PV scenario, reflecting the distribution of 91% wind and 9% PV capacity. Given that solar PV capacity in Ireland is low in 2023, and to explore how a more balanced distribution of wind and solar PV capacities might impact RES droughts, this study also considered a second scenario, referred to as 57W-43PV, where the installed solar PV capacity is assumed to increase to 8.6 GW, while wind capacity rises to 11.45 GW. These values are based on targets outlined in the roadmap published by the 2024 Climate Action Plan [23]. This study does not include offshore wind in the analysis. Recent reports suggest that even by 2030, Ireland is unlikely to have any significant new offshore wind farms, with projected offshore capacity expected to remain near zero using realistic scenarios [24].

New time series were generated for both the Atlite and C3S-E G solar PV datasets, incorporating a revised distribution of installed capacity across Ireland as specified in the roadmap. For wind power, the CF time series remains unchanged, as significant shifts in the location of wind farms are not expected. In total, twelve CF time series were analysed in this study, six for individual wind and solar PV CF (three datasets for each source) in the 91W-9PV scenario, and an additional six time series that include the combined CF for 91W-9PV and 57W-43PV scenarios across the different datasets.

It is important to note that the specific capacity values used in this study are illustrative and are not intended to reflect precise future realities. Instead, they serve to explore the impact of transitioning from a wind-dominated system (91W-9PV) to a more evenly distributed system (57W-43PV). This approach allows for a comparative analysis between the two scenarios, assessing how the balance of RES capacity affects the occurrence of RES droughts.

For each dataset (Atlite, C3S-E G, and C3S-E N), four distinct scenarios are examined, as summarised below:

- Wind Power / 91W-9PV
- Solar PV Power / 91W-9PV
- Combined RES / 91W-9PV
- Combined RES / 57W-43PV

### 3.5. RES Drought Definition

In this study, a RES drought event was defined as occurring when the 24-hour moving average of CF remains below a fixed threshold of 0.1 for

217 a period of longer than 24 hours. The choice of this threshold is somewhat  
 218 arbitrary, but aligns with similar studies on low renewable energy production  
 219 [4, 6, 7]. By using a 24-hour moving average, fewer but longer-lasting events  
 220 were captured compared to using the raw CF time series, which can be more  
 221 sensitive to short-term fluctuations. A fixed threshold approach was chosen  
 222 in this study to enable consistent inter-comparison between datasets.

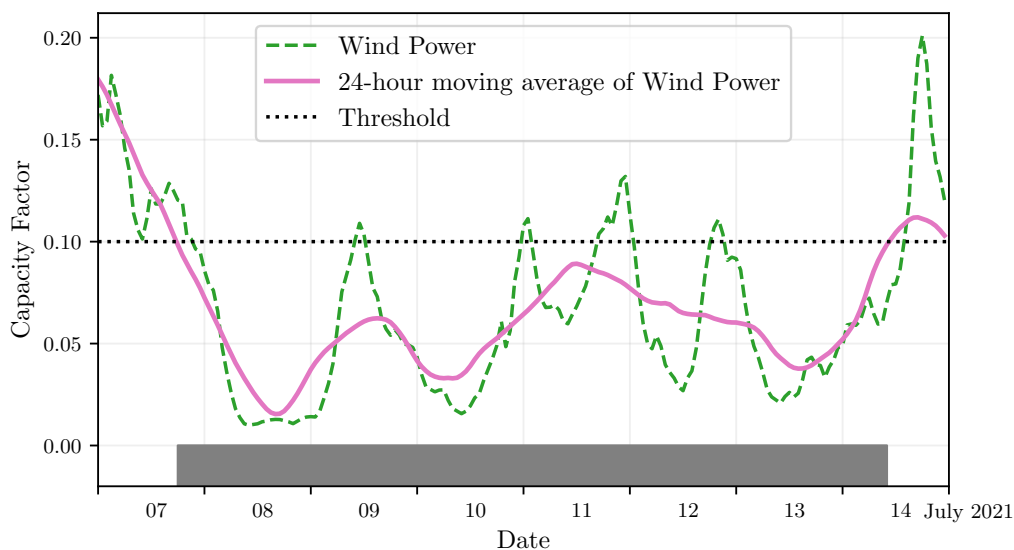


Figure 1: Wind time series of CF (green) and its 24-hour moving average (pink) from the 7th to the 15th of July 2021. The black dashed line indicates the CF threshold. The grey bar shows the period identified as a wind drought under our definition

223 The moving average approach smooths out short-term fluctuations, so  
 224 that brief periods above the threshold do not interrupt an otherwise con-  
 225 tinuous low-CF period (Fig. 1). This means that a single hour above the  
 226 threshold does not "break" a drought event if it is surrounded by prolonged  
 227 low-generation hours. As a result, fewer but longer-lasting drought events  
 228 are identified, which may better reflect real-world conditions where energy  
 229 supply constraints persist over extended periods.

## 230 4. Results

### 231 4.1. Verification

232 The accuracy of the datasets used in this study was verified, before con-  
233 tinuing to the analysis of RES droughts. For the verification process, time-  
234 varying values of installed capacity were used to account for changes in RES  
235 development over the verification period. This step allowed us to assess how  
236 well the datasets represent the production of renewable energy by comparing  
237 them against observed data.

#### 238 4.1.1. Wind Energy

239 The C3S-E datasets use the Vestas V136/3450 wind turbine power curve,  
240 (Fig. 2a). The Atlite model allows the user to specify the power curve.  
241 We considered the 121 power curves available for download from Renew-  
242 ables.ninja [22]. For each power curve, Renewables.ninja also provides four  
243 associated smoothed power curves. The smoothing is done using a Gaussian  
244 filter with different standard deviations that depend on the wind speed. A  
245 separate wind CF time series for Ireland was generated for each of the wind  
246 turbine power curves and smoothing levels.

247 The performance of each CF time series is then assessed based on four skill  
248 scores: correlation coefficient (CC), root mean square error (RMSE), mean  
249 bias error (MBE), and the percentage of overlap. The percentage of overlap  
250 quantifies the similarity between the observed and modelled distributions. It  
251 is a positively oriented skill score, where 100% shows full agreement between  
252 the two distributions, and 0% indicates no overlap. The histograms of hourly  
253 CF values for the most recent decade (2014-2023) are used to calculate this  
254 skill score.

255 Based on these metrics, the most representative power curve for Ireland  
256 is the Enercon E112.4500 power curve with the  $0.3w$  smoothing filter. The  
257 smoothing of the wind turbine power curve represents losses associated with  
258 each turbine, as well as losses such as wake effects between turbines, which  
259 are important when modelling wind energy on larger spatial scales. The his-  
260 togram in Fig. 2b shows that the C3S-E power curve tends to underestimate  
261 low CF values and overestimate higher ones, whereas the smoothed Atlite  
262 power curve more closely follows the observed wind availability data. This  
263 is further supported by the percentage of overlap which is higher for Atlite  
264 (97.2%) than for C3S-E (83.2%), indicating better agreement with observed  
265 data.

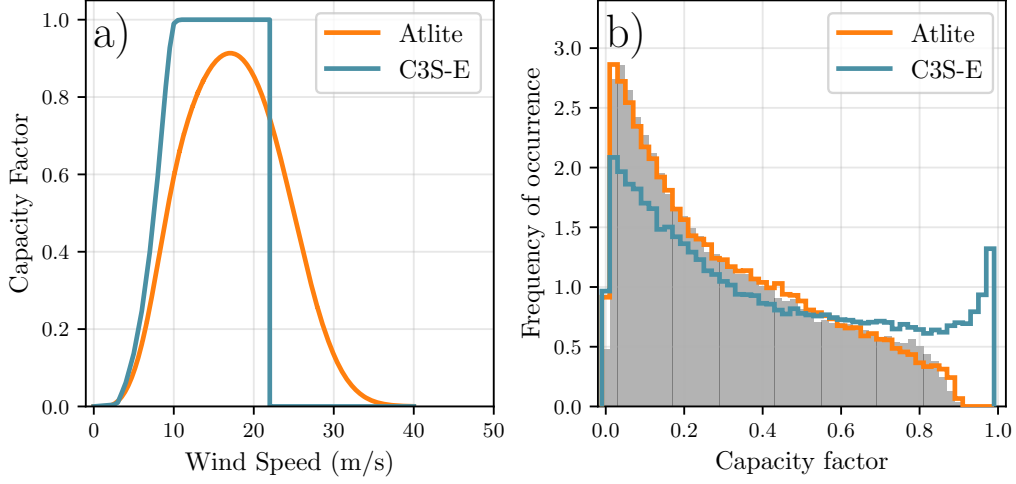


Figure 2: a) Power curves of the Enercon E112.4500 with a 0.3w smoothing filter used by Atlite (orange) and the Vestas V136/3450 used by C3S-E (blue) b) Histograms of wind CF for Ireland from Atlite (orange), C3S-E (blue) and Observed (shaded)

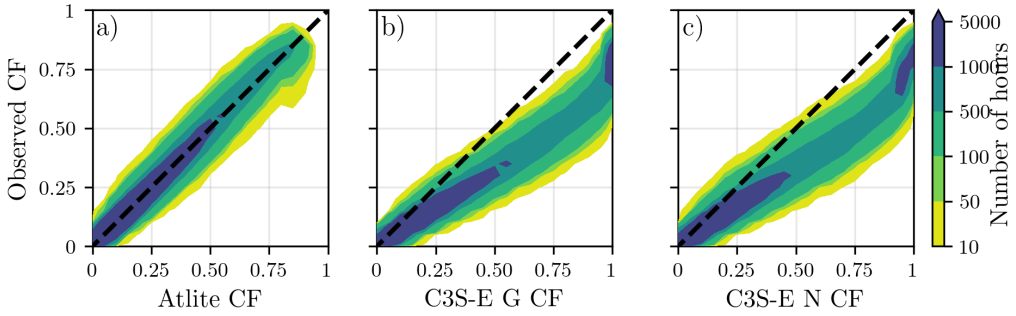


Figure 3: Wind CF density plot of the observed CF (vertical axes) and modelled (horizontal axes) CF data for the a) Atlite, b) C3S-E G and c) C3S-E N datasets

266 The effect of the difference between the power curves is also visible in  
 267 Fig. 3, which shows a density plot of wind CF values. The two C3S-E datasets  
 268 are shown to overestimate the observed CF, whereas the Atlite model is in  
 269 good agreement with the observed data. The skill scores presented in Table 2  
 270 show that Atlite performs better than the C3S-E datasets for all of the skill  
 271 scores.

272 Fig. 4 shows the average annual number of wind drought events during

	Atlite	C3S-E G	C3S-E N
<b>CC</b>	0.981	0.972	0.970
<b>RMSE</b>	0.045	0.177	0.162
<b>MBE</b>	-0.003	0.137	0.121

Table 2: Skill scores for wind power for the three datasets compared to observed data

the 2014 to 2023 validation period. The figure reveals that Atlite presents the best overall agreement with the observed frequency and duration of wind drought events. This pattern is particularly evident for shorter-duration events, which are the most frequent.

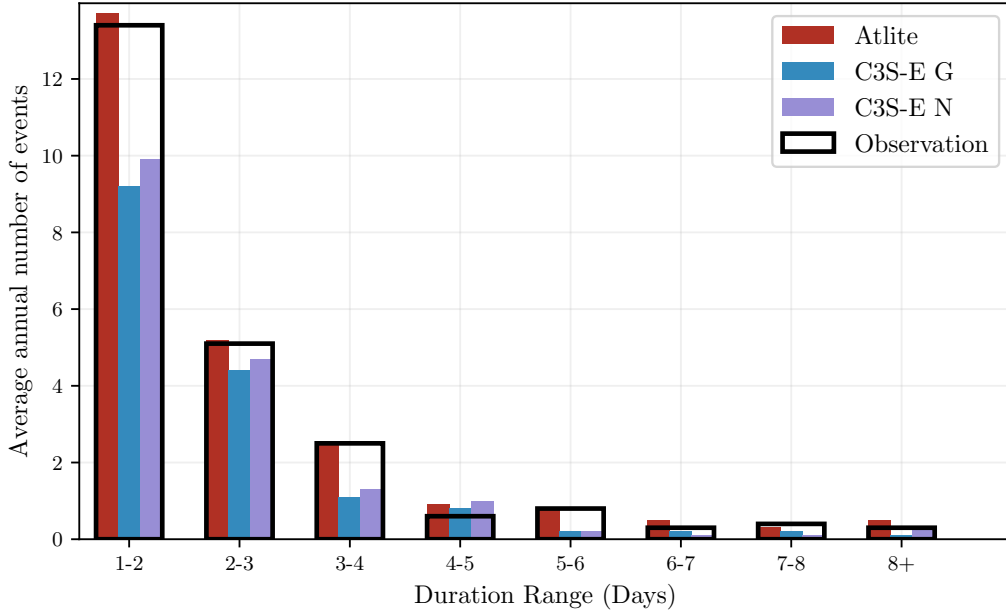


Figure 4: Average annual number of wind drought events for Atlite (red), C3S-E G (blue), C3S-E N (purple), and the observed data (black outline). The wind droughts are identified from 2014 to 2023, considering the actual capacity of the system at any given time

#### 4.1.2. Solar PV Energy

The Atlite model allows the user to select certain PV panel characteristics. In this study, the three PV panel types available in the Atlite model were considered (CSi, CdTe, Kaneka). Following the same methodology as in the

previous section, the three available models were compared using four skill scores (CC, RMSE, MBE, and the percentage of overlap). Based on the best-performing metrics, the Beyer PV panel model was selected [25], using the Kaneka Hybrid panel option. For all solar PV farm locations, the azimuth angle is fixed at  $180^\circ$  (due south), and the optimal tilt angle option is applied.

The solar PV installed capacity available on the spreadsheets from EirGrid represents the Maximum Export Capacity (MEC) and does not accurately reflect the installed solar PV capacity. To enable actual solar PV generation potential to be modelled correctly, installed capacities were set at 1.4 times the MEC values. This scaling factor was estimated by analysing proprietary data from individual solar PV farms provided by EirGrid, which showed that, on average, assuming that the installed capacities of farms exceed their MEC values by 40% yields the best agreement with the observed availability.

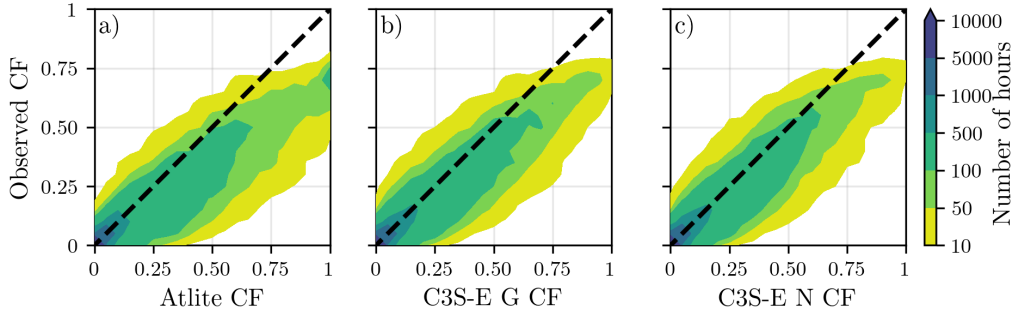


Figure 5: Solar PV CF density plot of the observed (vertical axes) and modelled (horizontal axes) CF series for the a) Atlite, b) C3S-E G and c) C3S-E N datasets

Figure 5 shows that the three datasets have a similar tendency to overestimate the CF compared to the observed values, especially for high CF values. The skill scores presented in Table 3 indicate that C3S-E G performs best overall, with the lowest RMSE and a high correlation coefficient, suggesting a closer match to observed data. All models show a slight positive bias, with Atlite exhibiting a slightly lower correlation and higher RMSE.

Fig. 6 shows the number of solar PV drought events during the 2023 validation period across different duration ranges. The figure reveals partial agreement between the three datasets and the observed data, with consistent results noticed for duration ranges of 1-2, 3-4, 7-8, and 8+ days. However, discrepancies appear in the other ranges, where the models diverge from the

	Atlite	C3S-E G	C3S-E N
<b>CC</b>	0.921	0.931	0.931
<b>RMSE</b>	0.119	0.090	0.113
<b>MBE</b>	0.046	0.027	0.021

Table 3: Skill scores for Solar PV CF for the three datasets compared to observed data

306 observed data. The main challenge in validating solar PV data stems from  
307 the recent installation of a large share of Ireland’s solar PV capacity, with  
308 over 65% of the total solar PV capacity installed in 2023. This results in  
309 uncertainties in solar PV generation data and the actual generating capacity  
310 in the first few months after each farm is connected.

311 As the goal of this analysis is to assess the combination of wind and solar  
312 PV generation, the complementary nature of these energy sources mitigates  
313 the limitations in solar PV-only results.

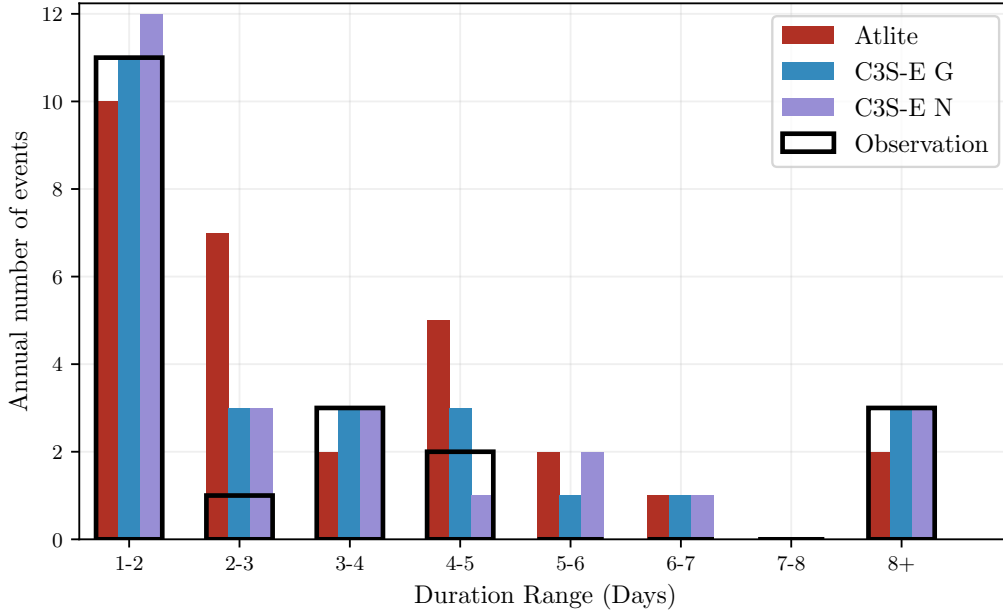


Figure 6: Number of solar PV drought events for Atlite (red), C3S-E G (blue), and C3S-E N (purple) and the observed data (black outline). The solar PV droughts are identified for 2023, considering the actual capacity of the system at any given time

## 314 4.2. Analysis

315 In this section, RES drought events are evaluated under two different  
316 scenarios with fixed installed capacities: the 91W-9PV scenario, with 5.9  
317 GW of wind capacity and 0.6 GW of solar PV capacity; and the 57W-43PV  
318 scenario, where wind capacity comprises 11.45 GW and solar PV capacity  
319 increases to 8.6 GW. Both scenarios were driven by 45 years of ERA5 data.  
320 Using the RES drought identification process described in Section 3.5, wind  
321 and solar PV droughts are first analysed separately before presenting the  
322 results for combined (wind + solar PV) RES droughts under both scenarios.

323 It is important to highlight that this analysis considers two key aspects:  
324 the absolute values that characterise RES droughts, which are crucial for  
325 power system planning, and the relative differences observed when comparing  
326 the various datasets and energy scenarios described in Section 3.4.

### 327 4.2.1. Annual Number of RES Droughts

328 The analysis of annual RES drought events reveals trends that are largely  
329 consistent with earlier studies. When only wind energy is considered (Fig.7a),  
330 the number of drought events decreases as the duration range increases, with  
331 very few events lasting more than seven days. This pattern aligns with  
332 previous research showing that wind droughts tend to be short and frequent.  
333 In contrast, for solar PV energy (Fig.7b), drought frequency declines from one  
334 to eight days and then slightly increases for longer durations. This behaviour  
335 is attributable to Ireland’s high-latitude location, where reduced sunlight in  
336 winter (from November to March) leads to consistently low solar PV output.

337 Moreover, the comparison between wind and solar PV results indicates  
338 that the median, first, and third quartiles for solar PV are consistently higher  
339 than or equal to those for wind. This is expected, given that solar PV gen-  
340 eration is inherently lower, zero at night, and limited by the solar cycle, as  
341 observed in other studies. When wind and solar PV are combined under the  
342 91W-9PV scenario (Fig.7c), the results closely mirror those of wind alone,  
343 reaffirming wind’s dominance in the current energy mix. However, in the  
344 57W-43PV scenario (Fig.7d), a marked reduction in drought events is ob-  
345 served across all datasets, with a decrease of the total number of events of  
346 56% for Atlite, 52% for C3S-E G, and 50% for C3S-E N, demonstrating the  
347 beneficial effects of a more balanced energy mix. These findings are in line  
348 with earlier studies that highlight how increasing solar PV capacity can miti-  
349 gate drought frequency through the anti-correlated seasonal patterns of wind  
350 and solar generation.



351 Additionally, the consistently higher drought counts reported by the Atlite  
 352 dataset, compared to the C3S-E datasets, underscore the impact of model  
 353 selection, particularly the influence of wind turbine power curve represen-  
 354 tation, on quantifying RES droughts. This observation is consistent with  
 355 previous research, which has also noted that assumptions regarding turbine  
 356 characteristics can significantly affect drought duration estimates.

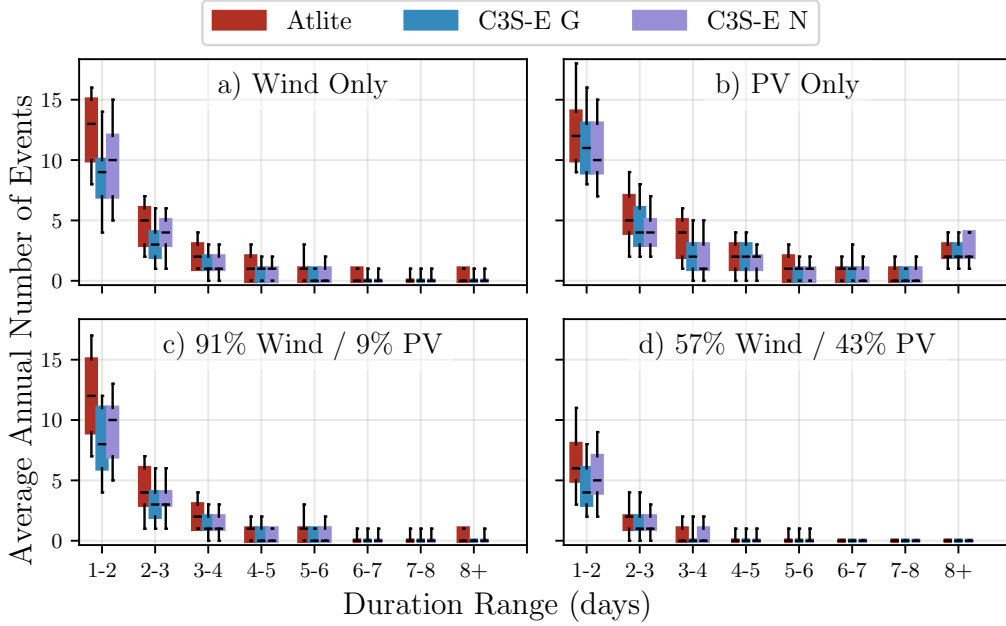


Figure 7: Average annual number of RES droughts (from 1979 to 2023) for a) Wind, b) solar PV, c) 91W-9PV and d) 57W-43PV for Atlite (red), C3S-E G (blue), and C3S-E N (purple). The x-axis represents duration ranges in days (lower bound included), while the y-axis indicates the annual number of events. The boxes display the first and third quartiles and the median is marked by a black line. The whiskers indicate the 5th and 95th percentiles

#### 357 4.2.2. Return Periods of RES Drought Duration

358 The RES drought events identified over the 45-year period were used to  
 359 calculate the return periods for different RES drought durations. A return  
 360 period is the estimated average time interval between events of a specified  
 361 duration or intensity (not to be confused with the frequency of their oc-  
 362 currence within a fixed time frame). Fig. 8 illustrates the return periods

for varying RES drought durations, highlighting how often different drought lengths are likely to occur across the datasets. This analysis not only quantifies the likelihood of prolonged low-generation periods but also provides insight into how extreme events are distributed across different timescales, helping to assess the variability of rare but impactful events. Understanding these return periods is crucial, as even infrequent droughts can challenge energy security by placing significant strain on conventional backup sources necessary to maintain supply in high-RES scenarios.

For wind (Fig. 8a), the log-linear increase in return periods observed in this study confirms that longer droughts occur exponentially less frequently, a trend consistent with earlier research on wind variability. In the case of solar PV droughts (Fig. 8b), the Atlite dataset shows a general log-linear trend, whereas the C3S-E datasets exhibit a sudden increase in drought duration for events exceeding sixteen days. This abrupt rise reflects differences in how solar PV output is handled near the CF threshold during low irradiance conditions. In the balanced scenario, the reduced share of wind and increased share of solar PV leverages their complementary seasonal patterns, resulting in higher return periods for combined drought events. This outcome highlights the benefit of a diversified energy mix in enhancing system resilience.

Under the 91W-9PV scenario (Fig. 8c), the combined RES drought return periods largely mirror those for wind alone, reflecting the dominance of wind in the current energy mix. In contrast, the balanced 57W-43PV scenario (Fig. 8d) shows a dramatic increase in return periods across all durations, suggesting that a more diversified energy mix can substantially mitigate the frequency of prolonged drought events.

Across Fig. 8a, c, and, d, the return periods in the Atlite dataset are consistently higher than those in the two C3S-E datasets. For instance, in the 91W-9PV scenario (Fig. 8c), an event with a one-year return period lasts six days in the Atlite dataset, compared to only five days in the C3S-E datasets. This difference underscores the importance of model selection when quantifying RES droughts, as each dataset's assumptions and parametrisations significantly influence drought duration estimates. Additionally, in all four graphs, the similarity between results from the two C3S-E datasets suggests that assumptions in the Atlite dataset, such as wind turbine power curve selection and PV panel specifications, have a greater impact on RES drought duration estimates than the precise geographic distribution of RES farms when studying the return periods of RES droughts.

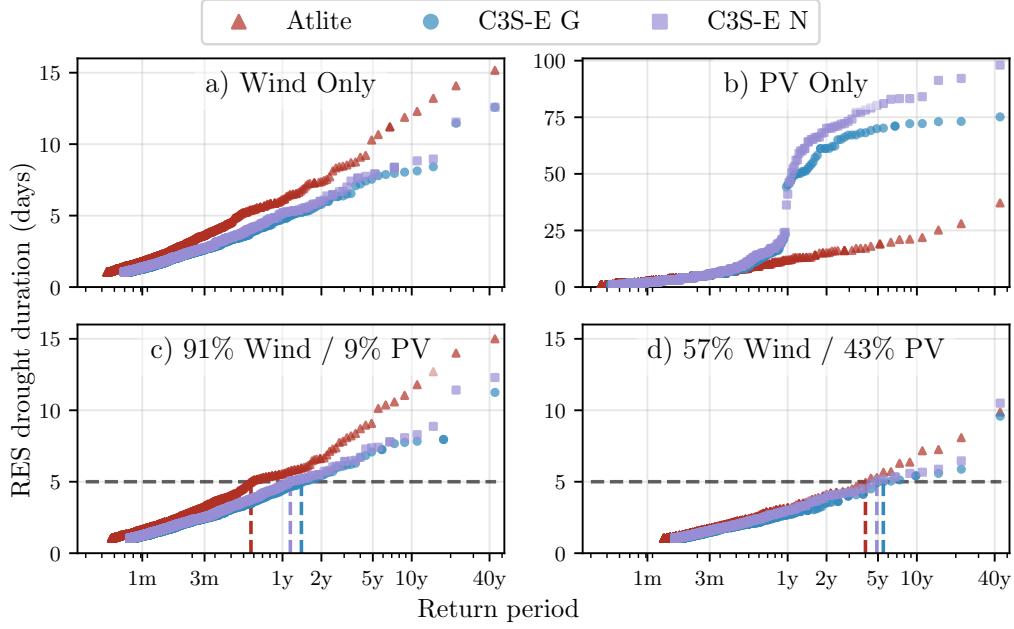


Figure 8: Return periods of the duration of RES droughts (from 1979 to 2023) for a) Wind, b) Solar PV, c) 91W-9PV and d) 57W-43PV for Atlite (red triangle), C3S-E G (blue circle), and C3S-E N (purple square). The x-axis represents the return period time in a log-scale and the y-axis indicates the duration of RES drought associated with it. The horizontal dashed line marks the 5-day return period, with coloured vertical dashed marking its return period for each dataset

#### 4.2.3. Seasonal Distribution of RES Droughts

The seasonal analysis of RES droughts is based on the percentage of hours in each month classified as drought events. Wind droughts tend to be more frequent during summer, whereas solar PV droughts are more common in winter due to reduced sunlight. By comparing these seasonal patterns across different datasets and energy scenarios, the study examines how model-specific assumptions and variations in capacity mix affect the overall characterisation of drought events.

For the wind-only scenario (Fig. 9a), the Atlite dataset exhibits a pronounced seasonal pattern, with about 24% of summer hours (June–July–August) identified as droughts compared to only 4% in winter (December–January–February). This strong seasonal signal is less evident in the C3S-E datasets, which suggests that the differences in the underlying wind power curves play a signifi-

cant role. In Atlite, CF near or below the 0.1 threshold occurs at relatively  
 higher wind speeds, resulting in a higher count of drought hours during the  
 summer months. In contrast, solar PV droughts (Fig. 9b) display an opposite  
 seasonal trend. Across all datasets, over 60% of winter hours are classified  
 as solar PV droughts, reflecting the naturally low solar irradiance in Ireland  
 during winter. Moreover, Atlite tends to record a slightly higher percentage  
 of drought hours for wind and a marginally lower percentage for solar PV rel-  
 ative to the C3S-E datasets. These differences highlight how dataset-specific  
 assumptions, such as the treatment of wind turbine power curves and PV  
 panel characteristics, significantly influences the apparent seasonal dynamics  
 of RES droughts.

The 91W-9PV scenario (Fig. 9c) shows patterns comparable to the ones  
 for wind droughts (Fig. 9a). However, in the 91W/9PV scenario, the number  
 of hours classified as RES droughts in summer decreases slightly compared to  
 the wind-only scenario. This reduction can be explained by the contribution  
 of solar PV generation during the summer months in the 91W-9PV scenario,  
 even though it constitutes only 11% of total capacity. Since the number of  
 RES drought hours for solar PV in summer is near zero, this small contribu-  
 tion has a noticeable impact on reducing overall drought hours. In the 57W-  
 43PV scenario (Fig. 9d), all three datasets show a reduction in monthly RES  
 drought frequency. Annual reductions in median RES drought frequency are  
 observed across the datasets, dropping from 14% to 5% for Atlite, from 8% to  
 3% for C3S-E G, and from 9% to 4% for C3S-E N. The balanced mix of wind  
 and solar PV power in this scenario reduces the seasonal signal overall and  
 significantly decreases the percentage of RES drought hours in the summer.

The seasonal variations observed in this study have important implica-  
 tions for energy planning. Given that energy demand peaks in winter for  
 Northern European countries, understanding these seasonal patterns is criti-  
 cal for assessing the need for conventional backup or storage solutions during  
 periods of prolonged low renewable output. The findings underscore that  
 even small differences in model assumptions leads to significant variations in  
 drought estimates, thereby affecting the reliability of the energy system dur-  
 ing critical periods. Such insights are essential for policymakers to develop  
 targeted strategies that enhance grid resilience and ensure a stable energy  
 supply throughout the year.

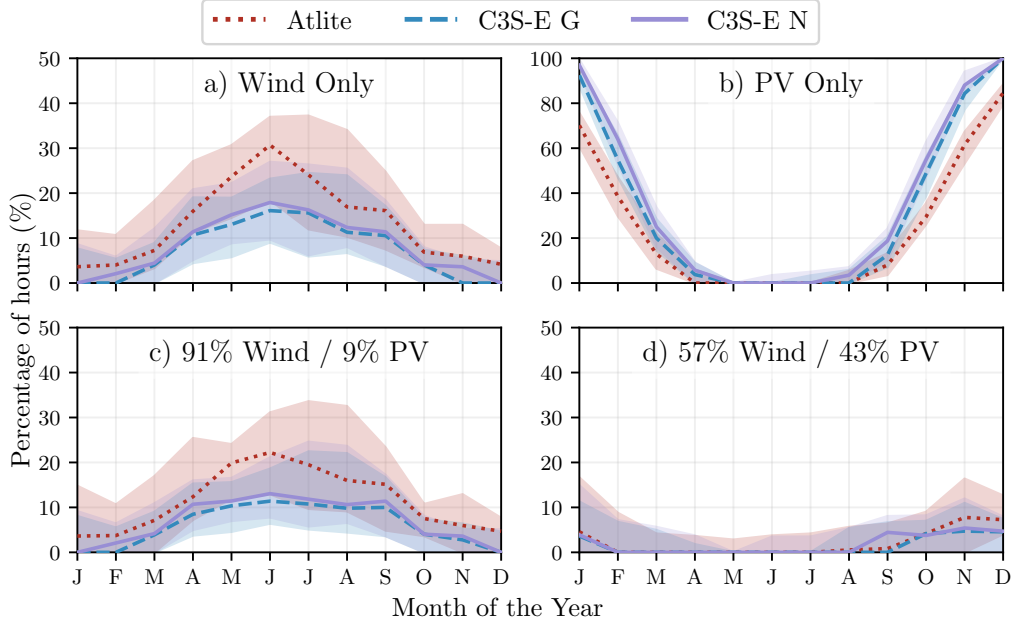


Figure 9: Percentage of hours in a month which are part of a RES drought (from 1979 to 2023) for a) Wind, b) Solar PV, c) 91W-9PV and d) 57W-43PV for Atlite (red dotted), C3S-E G (blue dashed), and C3S-E N (purple solid). The x-axis represents the month of the year, and the y-axis indicates the percentage of hours. Lines correspond to the median values and the area between the first and third quartiles is shaded. Note the different y-axis scale for b).

## 5. Conclusions

This study has investigated the ability of three RES datasets to represent RES droughts: Atlite, C3S-E G, and C3S-E N. One of the most evident differences is how each dataset incorporates the specific locations of RES farms. Both Atlite and C3S-E G consider the locations of wind and solar PV farms, which one would expect to result in a more accurate representation of RES generation. While this approach slightly improves solar PV models, our analysis indicates that for wind energy, the Atlite dataset performs better overall, especially in its close alignment with observed data for wind generation estimates. This finding suggests that, although the inclusion of RES farm locations is beneficial, the accuracy of the RES dataset is more strongly influenced by underlying model assumptions, such as selecting an appropriate wind power curve.

461 Atlite shows the best alignment with observed data for wind generation.  
462 Differences between the datasets are smaller for solar PV, with C3S-G per-  
463 forming marginally better than the other two. The results show that the  
464 two C3S-E datasets (C3S-E G and C3S-E N) consistently yield similar out-  
465 comes, indicating that their methodological differences have minimal impact  
466 in this case. This distinction is also evident in the analysis, where Atlite  
467 reports higher return periods and a greater number of RES droughts, espe-  
468 cially in scenarios with a balanced share of RES. Again, the results from RES  
469 drought modelling rely more on the precision of the wind power curve and  
470 PV panel models than on the specific locations of RES farms. Atlite’s supe-  
471 rior performance highlights the importance of selecting validated models for  
472 assessing RES drought risks. This careful model selection can better quantify  
473 risks, support effective planning, and avoid the potential underestimation of  
474 capacity needs, which is essential for ensuring energy security.

475 Looking at the 57W-43PV scenario, the analysis showed a significant im-  
476 provement in the management of RES droughts due to the complementary  
477 nature of wind and solar PV generation. Wind and solar PV together perform  
478 better in terms of reducing drought frequency and duration than either would  
479 individually, largely because of the seasonal anti-correlation between the two  
480 energy sources. This diversification reduces the seasonal impact on RES  
481 droughts, as solar PV generation peaks in the summer and wind generation  
482 is more consistent in winter. Ireland currently has a highly wind-dependent  
483 energy system, but with ambitious targets for solar PV installations in the  
484 coming years, the energy mix is expected to approach a balance between wind  
485 and solar PV capacity. While this balanced approach offers a more stable  
486 and secure energy supply by mitigating RES drought risks, it is important  
487 to note that having similar wind and solar PV capacities may not optimise  
488 other aspects, such as annual energy production or meeting nighttime loads.  
489 For policymakers, these findings underscore the importance of meeting these  
490 capacity targets to enhance energy security through diversification. Addition-  
491 ally, the choice of model for RES drought assessment becomes increasingly  
492 critical as more renewable capacity is integrated into the system.

493 This study has several limitations. Although ERA5 is among the best  
494 reanalysis datasets for renewable energy analysis, its resolution may not cap-  
495 ture local-scale phenomena, making it less reliable at the individual farm  
496 level. In addition, previous studies have indicated biases in ERA5 variables  
497 especially wind speed. Moreover, the methodology employs a fixed threshold  
498 to define RES drought events, which is necessary for comparing the three

models but does not account for demand variations. Consequently, while this approach enables a consistent inter-comparison, it may overlook events that are most critical for power system operations.

Future work is planned to extend the current analysis. First, climate projection data will be integrated with different energy scenarios, incorporating the addition of offshore wind, to better understand how climate change might affect RES droughts. Second, expanding the geographic domain of the study to include the rest of Europe would provide a more comprehensive understanding of RES droughts in an interconnected energy grid. This would require extensive verification across other European countries, making it a more complex but highly relevant challenge.

## Data Availability

The ERA5 data can be obtained from the Climate Data Store (<https://doi.org/10.24381/cds.adbb2d47>). The C3S-E dataset is also available from the Climate Data Store (<https://doi.org/10.24381/cds.4bd77450>). Information on wind and solar PV farms in Ireland can be obtained from the EirGrid website (<https://www.eirgrid.ie/grid/system-and-renewable-data-reports>). The Atlite model used in this study is open-source and can be found on GitHub (<https://github.com/pypsa/atlite>). The data and code required to reproduce the analysis in this article will be made available upon acceptance of the manuscript in a public GitHub repository.

## Acknowledgments

The research conducted in this publication was funded by Science Foundation Ireland and co-funding partners under grant number 21/SPP/3756 through the NexSys Strategic Partnership Programme.

## References

- [1] EuroStat, Renewable Energy Statistics, 2023. URL: [https://ec.europa.eu/eurostat/statistics-explained/index.php?title=Renewable\\_energy\\_statistics](https://ec.europa.eu/eurostat/statistics-explained/index.php?title=Renewable_energy_statistics), Accessed: 2024-11-06.
- [2] H. C. Bloomfield, D. J. Brayshaw, L. C. Shaffrey, P. J. Coker, H. E. Thornton, Quantifying the increasing sensitivity of power systems to

- 530 climate variability, *Environmental Research Letters* 11 (2016) 124025.  
531 doi:10.1088/1748-9326/11/12/124025.
- 532 [3] H. C. Bloomfield, D. J. Brayshaw, A. Troccoli, C. M. Goodess, M. De Fe-  
533 lice, L. Dubus, P. E. Bett, Y.-M. Saint-Drenan, Quantifying the  
534 sensitivity of european power systems to energy scenarios and cli-  
535 mate change projections, *Renewable Energy* 164 (2021) 1062–1075.  
536 doi:10.1016/j.renene.2020.09.125.
- 537 [4] F. Kaspar, M. Borsche, U. Pfeifroth, J. Trentmann, J. Drücke, P. Becker,  
538 A climatological assessment of balancing effects and shortfall risks of  
539 photovoltaics and wind energy in germany and europe, *Advances in*  
540 *Science and Research* 16 (2019) 119–128. doi:10.5194/asr-16-119-2  
541 019.
- 542 [5] F. Mockert, C. M. Grams, T. Brown, F. Neumann, Meteorological  
543 conditions during periods of low wind speed and insolation in Germany:  
544 The role of weather regimes, *Meteorological Applications* 30 (2023)  
545 e2141. doi:10.1002/met.2141.
- 546 [6] M. Ohba, Y. Kanno, D. Nohara, Climatology of dark doldrums in japan,  
547 *Renewable and Sustainable Energy Reviews* 155 (2022) 111927. doi:10  
548 .1016/j.rser.2021.111927.
- 549 [7] M. J. Mayer, B. Biró, B. Szücs, A. Aszódi, Probabilistic modeling of  
550 future electricity systems with high renewable energy penetration using  
551 machine learning, *Applied Energy* 336 (2023) 120801. doi:10.1016/j.  
552 apenergy.2023.120801.
- 553 [8] D. Raynaud, B. Hingray, B. François, J. Creutin, Energy droughts from  
554 variable renewable energy sources in European climates, *Renewable*  
555 *Energy* 125 (2018) 578–589. doi:https://doi.org/10.1016/j.renene  
556 .2018.02.130.
- 557 [9] A. Gangopadhyay, A. K. Seshadri, N. J. Sparks, R. Toumi, The role  
558 of wind-solar hybrid plants in mitigating renewable energy-droughts,  
559 *Renewable Energy* 194 (2022) 926–937. doi:10.1016/j.renene.2022.  
560 05.122.
- 561 [10] J. Kapica, J. Jurasz, F. A. Canales, H. Bloomfield, M. Guezgouz,  
562 M. De Felice, Z. Kobus, The potential impact of climate change on



- 563 european renewable energy droughts, *Renewable and Sustainable En-*  
564 *ergy Reviews* 189 (2024) 114011. doi:10.1016/j.rser.2023.114011.
- 565 [11] K. Z. Rinaldi, J. A. Dowling, T. H. Ruggles, K. Caldeira, N. S. Lewis,  
566 Wind and Solar Resource Droughts in California Highlight the Benefits  
567 of Long-Term Storage and Integration with the Western Interconnect,  
568 *Environmental Science and Technology* 55 (2021) 6214–6226. doi:10.1  
569 021/acs.est.0c07848.
- 570 [12] P. T. Brown, D. J. Farnham, K. Caldeira, Meteorology and climatology  
571 of historical weekly wind and solar power resource droughts over western  
572 North America in ERA5, *SN Applied Sciences* 3 (2021) 814. doi:10.1  
573 007/s42452-021-04794-z.
- 574 [13] S. Allen, N. Otero, Standardised indices to monitor energy droughts,  
575 *Renewable Energy* 217 (2023) 119206. doi:10.1016/j.renene.2023.11  
576 9206.
- 577 [14] C. Bracken, N. Voisin, C. D. Burleyson, A. M. Campbell, Z. J. Hou,  
578 D. Broman, Standardized benchmark of historical compound wind and  
579 solar energy droughts across the Continental United States, *Renewable*  
580 *Energy* 220 (2024) 119550. doi:https://doi.org/10.1016/j.renene  
581 .2023.119550.
- 582 [15] H. Lei, P. Liu, Q. Cheng, H. Xu, W. Liu, Y. Zheng, X. Chen, Y. Zhou,  
583 Frequency, duration, severity of energy drought and its propagation in  
584 hydro-wind-photovoltaic complementary systems, *Renewable Energy*  
585 (2024) 120845. doi:10.1016/j.renene.2024.120845, 2.
- 586 [16] H. Hersbach, B. Bell, P. Berrisford, S. Hirahara, A. Horányi, J. Muñoz-  
587 Sabater, J. Nicolas, C. Peubey, R. Radu, D. Schepers, et al., The ERA5  
588 global reanalysis, *Quarterly Journal of the Royal Meteorological Society*  
589 146 (2020) 1999–2049. doi:10.1002/qj.3803.
- 590 [17] L. Dubus, Y. Saint-Drenan, A. Troccoli, M. De Felice, Y. Moreau, L. Ho-  
591 Tran, C. Goodess, R. Amaro E Silva, L. Sanger, C3S Energy: A climate  
592 service for the provision of power supply and demand indicators for Eu-  
593 rope based on the ERA5 reanalysis and ENTSO-E data, *Meteorological*  
594 *Applications* 30 (2023) e2145. doi:10.1002/met.2145.

- 595 [18] F. Hofmann, J. Hampp, F. Neumann, T. Brown, J. Hörsch, Atlite: a  
596 lightweight Python package for calculating renewable power potentials  
597 and time series, *Journal of Open Source Software* 6 (2021) 3294. doi:10  
598 .21105/joss.03294.
- 599 [19] EirGrid & SONI, System and Renewable Data Reports, 2023. URL:  
600 [https://www.eirgrid.ie/grid/system-and-renewable-data-rep](https://www.eirgrid.ie/grid/system-and-renewable-data-reports)  
601 [orts](https://www.eirgrid.ie/grid/system-and-renewable-data-reports), Accessed: 2024-11-06.
- 602 [20] E. Doddy Clarke, S. Griffin, F. McDermott, J. Monteiro Correia,  
603 C. Sweeney, Which reanalysis dataset should we use for renewable en-  
604 ergy analysis in ireland?, *Atmosphere* 12 (2021) 624. doi:10.3390/atmo  
605 s12050624.
- 606 [21] Y.-M. Saint-Drenan, L. Wald, T. Ranchin, L. Dubus, A. Troccoli, An  
607 approach for the estimation of the aggregated photovoltaic power gener-  
608 ated in several European countries from meteorological data, *Advances*  
609 *in Science and Research* 15 (2018) 51–62. doi:10.5194/asr-15-51-201  
610 8.
- 611 [22] I. Staffell, S. Pfenninger, Using bias-corrected reanalysis to simulate  
612 current and future wind power output, *Energy* 114 (2016) 1224–1239.  
613 doi:10.1016/j.energy.2016.08.068.
- 614 [23] Government of Ireland, Climate Action Plan 2024, Technical Report 3,  
615 Department of the Environment, Climate and Communications, 2023.  
616 URL: [https://www.gov.ie/pdf/?file=https://assets.gov.ie/](https://www.gov.ie/pdf/?file=https://assets.gov.ie/284675/70922dc5-1480-4c2e-830e-295afd0b5356.pdf)  
617 [284675/70922dc5-1480-4c2e-830e-295afd0b5356.pdf](https://www.gov.ie/pdf/?file=https://assets.gov.ie/284675/70922dc5-1480-4c2e-830e-295afd0b5356.pdf), Accessed:  
618 2024-11-06.
- 619 [24] Sustainable Energy Authority Ireland, National Energy Projections  
620 2024, Technical Report, Sustainability Energy Authority of Ireland,  
621 2024. URL: [https://www.seai.ie/news-and-events/news/energ](https://www.seai.ie/news-and-events/news/energy-projections-report)  
622 [y-projections-report](https://www.seai.ie/news-and-events/news/energy-projections-report), Accessed: 2024-11-06.
- 623 [25] H. G. Beyer, G. Heilscher, S. Bofinger, A robust model for the mpp  
624 performance of different types of pv-modules applied for the performance  
625 check of grid connected systems, *Eurosun* (2004) 8.